H_∞ ROBUST CONTROL DESIGN FOR A LARGE FLEXIBLE AIRCRAFT

Costin ENE[1], Valentin PANA[2]

This paper focuses on improving in the dynamic response for the longitudinal channel of a large flexible aircraft similar to the Rockwell B-1 aircraft developed from the available literature data. The proposed approach is based on the H_∞ robust control problem with respect to NLCF and it is intended to provide good tracking of the desired pitch attitude while reducing the flexible modes effects. This control technique is implemented and tested on the resulted analogous nonlinear model of the Rockwell B-1 aircraft. A thorough robustness analysis and several simulations are performed in order to show the effectiveness of the proposed method.

Keywords: longitudinal dynamics; flexible modes; parametric uncertainty; NLCF; nonlinear model

1. Introduction

The Rockwell B-1 aircraft is a long-range strategic bomber with the ability to conduct terrain following missions. Fuel efficiency and large operational domains are two objectives often obtained by reducing the weight of the aircraft. This makes the structure more flexible and increases the susceptibility to aeroelastic phenomena. The common method to deal with adverse aeroelastic effects is to design flight control systems for the rigid body dynamics and then use filters in order to avoid these effects. This type of solution was implemented in [1] in order to alleviate the interactions between the flexibility of the aircraft and also the atmospheric turbulence. These types of interactions lead to handling qualities degradations and increased tracking errors because of the structural motion in the cockpit area. Thus, the authors in [1] address the two problems separately and use a dedicated automatic control system called *structural mode control system* (SMCS). It was conceived as a fail-safe and its design objective was to obtain a system that will not interact with regular control techniques used for the rigid body motion [2]. Handling qualities and crew efficiency caused by structural motion in the cockpit area of the fuselage were the two improvements.

[1] Asist. Prof., Univ., Dept.of Aeronautical System Engineering and Aeronautical Management "Nicolae Tipei", University POLITEHNICA of Bucharest, Romania, e-mail: costin.ene@upb.ro
[2] Lect., Univ., Dept.of Aeronautical System Engineering and Aeronautical Management "Nicolae Tipei", University POLITEHNICA of Bucharest, Romania, e-mail: valentin.pana@upb.ro

The above control design methods employ a procedure that addresses one control loop at a time in a cascaded order. Structural mode control systems [3] are placed in a different control loop ensuring a separation that prevents the interaction between conventional control surfaces and aeroelastic control and also between dedicated SMCS actuators and FCS operation.

The H_∞ control problem (see [4], [5], [6], [7]) or the γ-attenuation problem has been formulated for the first time in the early 1980's by Vidyasagar. A reason of its remarkable success is its capabilities to handle modeling uncertainties [9], [10]. There are mainly three types of uncertainties (each of them being treated in a specific way): additive uncertainties, multiplicative uncertainties and uncertainties with respect to the *normalized left coprime factorization* (NLCF). The third type of uncertainties was first addressed by Vidyasagar in 1985, later in the same decade by Duncan C. McFarlane and Keith Glover [7] in 1989. The present paper proposes a H_∞ control design with respect to NLCF that will combine both control objectives and allows interactions between all existing control surfaces in order to achieve both objectives (conventional control and elasticity effects minimization) simultaneously.

The paper is organized as follows: section 2 presents the linearized model of the Rockwell B-1 obtained from the nonlinear model described in [1] and [11], also adding parametric uncertainties affecting the rigid body and the elastic modes, section 3 presents the synthesis objectives and control design for each of the proposed method, section 4 provides a good robustness analysis of the linear model with respect to rigid body uncertainties and flexible modes uncertainties, section 5 presents the simulations for the nonlinear model and section 6 presents the concluding remarks and future work.

2. Model of a large flexible aircraft

The SIMULINK nonlinear model of the Rockwell B-1 aircraft was implemented from the available data in [1] and [11] and includes six rigid-body degrees of freedom plus five elastic degrees of freedom. This are the modes identified to be the most important regarding cockpit ride quality and flexible-rigid interactions [1]. Extensions to this initial model, proposed by David K. Schmidt, include additional aerodynamic modeling and a nonlinear model of the engine dynamics. The model contains the following control effectors: symmetric and antisymmetric horizontal tail deflections, wing spoilers, a split rudder, and control vanes for structural mode control. The rigid body equation of motion can be found in [1], as well as the first three symmetric modes which affect the longitudinal dynamics and the last two affecting lateral-directional dynamics. This paper will only focus on the longitudinal dynamics of the Rockwell B-1 aircraft. This paper keeps the same SI units used in [1] for distance, velocities, angular rates, angles etc.

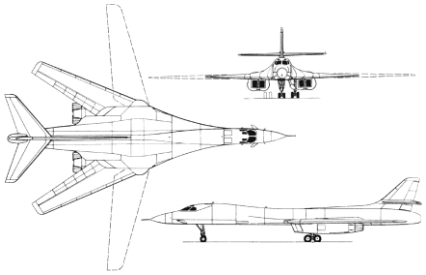

Fig. 1 Three-view of the Rockwell B-1 [1]

The SIMULINK nonlinear flexible model was trimmed for some initial conditions which include all states and control inputs. Thus, an equilibrium flight condition was obtained for level flight resulting in the following nominal flight conditions: true air speed $TAS = 658.74\ ft/s$, altitude $h = 5000\ ft$, angle of attack $\alpha = 0.0126\ rad$. After this a linearization procedure was applied such that the following linear longitudinal system was obtained:

$$\begin{aligned} \dot{x}(t) &= Ax(t) + B\delta(t) \\ y(t) &= Cx(t) + D\delta(t), \end{aligned} \tag{1}$$

where $x(t) = [u(t), w(t), q(t), \theta(t), \dot{\eta}_1(t), \dot{\eta}_2(t), \dot{\eta}_3(t), \eta_1(t), \eta_2(t), \eta_3(t)]^T$ is the state vector with components: forward velocity $u[ft/s]$, vertical velocity $w[ft/s]$, pitch rate $q\ [rad/s]$, pitch angle $\theta\ [rad]$, and the longitudinal flexible mode components given by η_1, η_2, η_3 and their derivatives $\dot{\eta}_1, \dot{\eta}_2, \dot{\eta}_3$. $\delta(t) = \left[\delta_{Hc}(t), \delta_{cvsym}(t)\right]^T$, represent the control inputs given by the symmetric horizontal tail $\delta_{Hc}\ [deg]$ and the symmetric vane deflection $\delta_{cvsym}\ [deg]$. The outputs vector is given by $y(t) = [u(t), w(t), q(t), \theta(t), a_z(t), \alpha(t), n_{zcg}(t), n_{zcp}(t)]^T$, where u, w, q, θ are the first four states, $a_z\ [ft/s^2]$ is the normal acceleration, $\alpha\ [rad]$ is the angle of attack. Usually, n_z is defined as a dimensionless load factor, but here, same as the authors in [1], $n_{zcg}\ [ft/s^2]$ is considered to be the normal acceleration adding the gravitational acceleration effect measured at the center of gravity and $n_{zcp}\ [ft/s^2]$ is the same normal acceleration (adding gravitational effect) but measured at the cockpit location.

The resulting linearized longitudinal system matrices are:

$$A = \begin{bmatrix} -0.014805 & 0.083948 & -10.061 & -32.167 & 0 & 0 & 0 & 0 & 0 & 0 \\ -0.091865 & -0.46092 & 673.58 & -0.40541 & -0.096782 & 1.1614 & 0.067806 & -2.8096 & 29.646 & 1.4532 \\ 7.4958e-05 & -0.0047222 & -0.94339 & 2.552e-08 & -0.0037082 & 0.029406 & 0.004128 & -0.065843 & -0.056491 & 0.084702 \\ 0 & 0 & 1 & 0 & 0 & 0 & 0 & 0 & 0 & 0 \\ 0.30968 & -1.6758 & -79.589 & 0 & -0.85361 & -0.16444 & 0.54814 & -153.78 & -6.4989 & 25.635 \\ 0.024365 & 0.053526 & 0.18686 & 0 & 0.13962 & -5.3435 & 0.067186 & 5.8223 & -325.47 & 2.7244 \\ -0.077539 & 0.21922 & 4.5854 & 0 & -0.072401 & 2.2535 & -0.84831 & 2.8912 & 14.307 & -451.61 \\ 0 & 0 & 0 & 0 & 1 & 0 & 0 & 0 & 0 & 0 \\ 0 & 0 & 0 & 0 & 0 & 1 & 0 & 0 & 0 & 0 \\ 0 & 0 & 0 & 0 & 0 & 0 & 1 & 0 & 0 & 0 \end{bmatrix},$$

$$B = \begin{bmatrix} 0.25739 & 0 \\ -0.73191 & -0.022283 \\ -0.093401 & 0.0021786 \\ 0 & 0 \\ -16.131 & -0.60788 \\ -1.5495 & -0.012474 \\ 4.4388 & -0.059742 \\ 0 & 0 \\ 0 & 0 \\ 0 & 0 \end{bmatrix}, \quad D = \begin{bmatrix} 0 & 0 \\ 0 & 0 \\ 0 & 0 \\ 0 & 0 \\ -0.73191 & -0.022283 \\ 0 & 0 \\ 0.18719 & 0.039596 \\ -2.7008 & -0.55784 \end{bmatrix},$$

$$C = \begin{bmatrix} 1 & 0 & 0 & 0 & 0 & 0 & 0 & 0 & 0 & 0 \\ 0 & 1 & 0 & 0 & 0 & 0 & 0 & 0 & 0 & 0 \\ 0 & 0 & 1 & 0 & 0 & 0 & 0 & 0 & 0 & 0 \\ 0 & 0 & 0 & 1 & 0 & 0 & 0 & 0 & 0 & 0 \\ -0.091865 & -0.46092 & 14.892 & -0.40541 & 0 & 0 & 0 & 0 & 0 & 0 \\ -1.9123e-05 & 0.0015179 & 0 & 0 & 0 & 0 & 0 & 0 & 0 & 0 \\ -0.11043 & -0.3364 & 21.505 & -4.211e-10 & -0.011269 & 0.90576 & 0.12027 & 10.684 & 28.514 & 53.339 \\ 0.065639 & -0.98503 & 36.427 & -1.7792e-06 & -0.28139 & -3.1815 & -0.20235 & -82.88 & -153.24 & -168.64 \end{bmatrix} \quad (2)$$

The longitudinal dynamics at this flight condition is stable. The stability characteristics have a damping factor $\zeta_s = 0.373$ and a natural frequency $\omega_s = 1.75\ rad/s$ for the short period, while for the phugoid we have $\zeta_p = 0.11$ and $\omega_p = 0.0654\ rad/s$. The other six high frequency poles are given by the flexible modes and they have values between $10\ rad/s < \omega_{flex} < 25\ rad/s$.

In order to improve the handling qualities, a state-feedback control law for δ_{Hc} SAS is designed having $K_q = -8.8645, K_\theta = -17.201$. The resulting system response improves significantly for the short period ($\zeta_s = 0.498$ and $\omega_s = 1.94\ rad/s$) and phugoid ($\zeta_p = 0.502$ and $\omega_p = 0.15\ rad/s$) mainly because of the increase of the damping and also one achieves a faster response by increasing the natural frequency of the phugoid. Even with the improved augmented system, the effect of the flexible modes to n_{zcg} and n_{zcp} can be seen in the first 10 *sec* of transient time when applying a step command to the control surfaces. The oscillations noted in Fig. 2(a) can only be the result of the low damped high frequency poles i.e., the ones corresponding to the flexible modes. One can notice that the effect from the δ_{cvsym} deflection is very small with respect to the δ_{Hc} input. Fig. 2(b) shows the augmented linear system affected by uncertainty for all the terms in the matrices $A\ and\ B$ from (2) that are different from 0 and 1. In total there are 63 uncertain terms taken into consideration with $\pm 10\%$ uncertainty. Fig. 2(b) shows the Pole-Zero Map of 100 systems contained within the specified bounds.

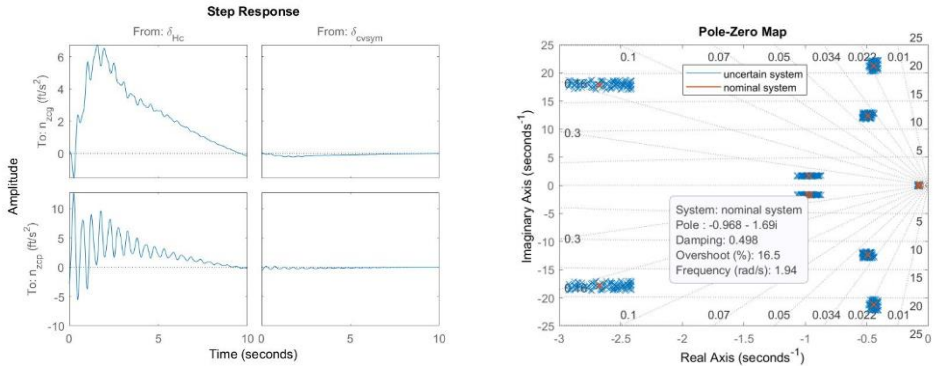

(a) Step response ($\delta_{Hc}\ and\ \delta_{cvsym}$ to n_{zcg} and n_{zcp}) (b) Pole-Zero Map of the uncertain system

Fig. 2 The augmented system characteristics

3. Robust control design and synthesis objective

In the following important key aspects related to H_∞ robust control problem with respect to NLCF.

For the rational transfer matrix $G(s)$ (representing the linearized dynamics of a plant) there exists $M\ and\ N$ (stable rational transfer matrices with M square and invertible) such that $G = M^{-1}N$. $M\ and\ N$ satisfy the propriety $MV - NU = I$, with U and V stable transfer functions and are called left coprime factorization of G. If $M\ and\ N$ satisfy the additional propriety $NN^* + MM^* = I$, they are called normalized left coprime factorization of G.

The dynamic stable uncertainty $\Delta = [\Delta_N \quad \Delta_M]$ is called coprime factor uncertainty if $G_\Delta = (M + \Delta_M)^{-1}(N + \Delta_N)$, where $M\ and\ N$ represent the NLCF of G. This representation and its equivalent can be seen in Fig. 3(a) and Fig. 3(b) respectively.

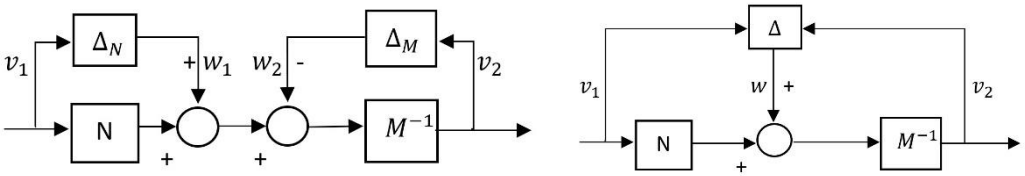

(a) Representation of $G_\Delta = (M + \Delta_M)^{-1}(N + \Delta_N)$ (b) Equivalent representation of G_Δ

Fig. 3 The uncertain system representation with respect to NLCF

When applying a controller to the uncertain system in Fig. 3 the resulting system can be seen in Fig. 4(a) and its equivalent in Fig. 4(b)

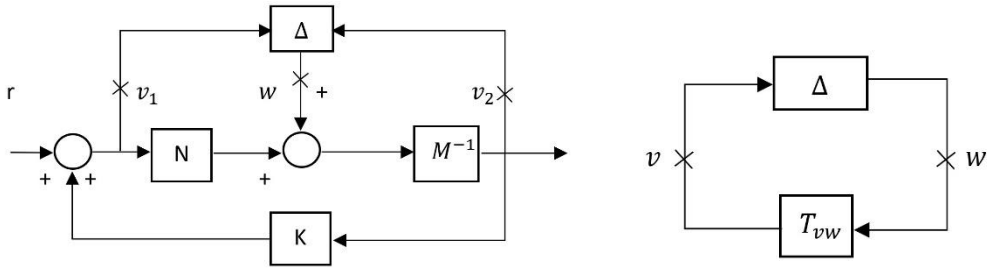

(a) NLCF control problem (b) Equivalent representation

Fig. 4 The uncertain system representation with respect to NLCF with controller

Computing v_1 and v_2 for T_{vw} yields:

$$v_1 = KM^{-1}(Nv_1 + w) \rightarrow v_1 = (I - KG)^{-1}KM^{-1}w$$
$$\rightarrow v_1 = K(I - GK)^{-1}M^{-1}w \quad (3)$$
$$v_2 = M^{-1}(w + NKv_2) \rightarrow v_2 = (I - GK)^{-1}M^{-1}w \quad (4)$$

The resulting generalized system having the output $v = \begin{bmatrix} v_2 \\ v_1 \end{bmatrix}$ and the input w is given by:

$$T_{vw} = \begin{bmatrix} (I - GK)^{-1} \\ K(I - GK)^{-1} \end{bmatrix} M^{-1} \quad (5)$$

From the Small Gain Theorem [7], the robustness condition with respect to NLCF is:

$$\left\| \begin{bmatrix} (I-GK)^{-1} \\ K(I-GK)^{-1} \end{bmatrix} M^{-1} \right\|_{\infty} < \delta^{-1}, \tag{6}$$

where K is the stabilizing controller of the system $G_{\Delta} = (M + \Delta_M)^{-1}(N + \Delta_N)$ with $\Delta = [\Delta_N \quad \Delta_M]$ and $\|\Delta\|_{\infty} < \delta$.

The generalized system corresponding to the H_{∞} control problem in the case where the nominal model G has $D = 0$ is given by:

$$\begin{bmatrix} M^{-1}(s) & \vdots & G(s) \\ 0 & \cdots & I \\ \cdots & \cdots & \cdots \\ M^{-1}(s) & \vdots & G(s) \end{bmatrix} := \left(A, [-H \quad B], \begin{bmatrix} C \\ 0 \\ \cdots \\ C \end{bmatrix}, \begin{bmatrix} I & \vdots & 0 \\ 0 & \vdots & I \\ \cdots & \cdots & \cdots \\ I & \vdots & 0 \end{bmatrix} \right). \tag{7}$$

One can notice that the lower linear fractional transformation for the left side of the above system is exactly T_{vw} in (5).

The proposed robust control design for the Rockwell B-1 aircraft presented in Chapter II has the following objectives:

- Ensure Level 1 handling qualities;
- Minimizing the tracking error between the output of a given ideal model H_m and the output measured pitch angle of the aircraft $\theta(t)$ for piecewise doublet type commands;
- Minimizing the tracking error $n_{zcp}(t) - n_{zcg}(t)$;
- Reduced sensitivity for the outputs $\theta(t), n_{zcp}(t)\ and\ n_{zcg}(t)$
- Robustness with respect to parametric uncertainties

In this example $G(s)$ is the transfer function with the state space representation given by $G(s) := (A_{SAS}, B, C_{meas}, D_{meas})$ where $A_{SAS} = A - B\begin{bmatrix} 0 & 0 & K_q & K_{\theta} \end{bmatrix}$ is the augmented A matrix and B the same as in (2), while the measured outputs $y_m = \begin{bmatrix} q, \theta, n_{zcg}, n_{zcp} \end{bmatrix}^T$ are obtained using the appropriate matrices C_{meas} and D_{meas}.

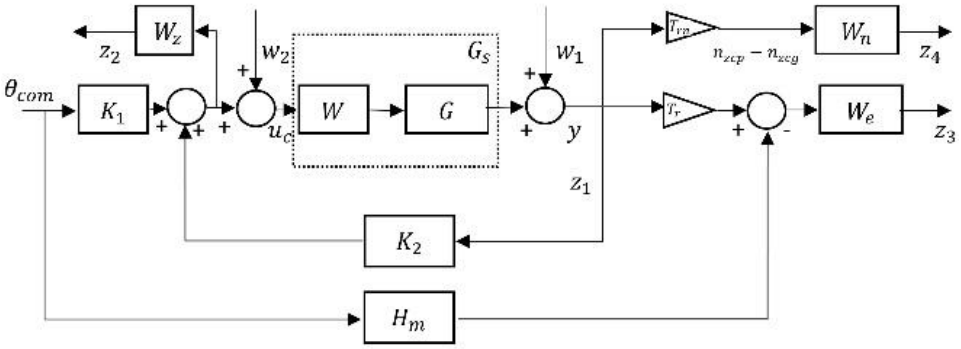

Fig. 6 Robust control configuration

The adopted control design represents a modified H_{∞} loop-shaping procedure with two degrees of freedom inspired from [5] and can be seen in Fig. 6 where:

- The exogenous inputs are: θ_{com}, w_1, w_2 where:
  - θ_{com} represents the desired pitch angle
  - w_1, w_2 are the inputs denoting the equivalent H_∞ robust control problem with respect to NLCF
- The control variable: u_c representing:
  - u_c represents the two control surfaces of the aircraft model $u_c = \left[\delta_{Hc}, \delta_{cvsym}\right]^T$
- The regulated outputs are: z_1, z_2, z_3, z_4 where:
  - z_1 represents the first set of regulated outputs given by the measured outputs of the aircraft, which in this case gives $z_1 = \left[\, q, \theta, n_{zcg}, n_{zcp}\right]^T$
  - z_2 represents the scaled output given by the controller $\left[\delta_{Hc}, \delta_{cvsym}\right]^T W_z$, where $W_z = \begin{bmatrix} 19.5 & 0 \\ 0 & 1.2 \end{bmatrix}$
  - z_3 represents the scaled output given by $z_3 = (y_m T_r - \theta_{com} H_m) W_e$, where:
    - T_r is a matrix with linear independent rows so that one can select θ from the measured variables vector y_m given by: $T_r = [0 \;\; 1 \;\; 0 \;\; 0]$
    - H_m is an ideal transfer function chosen from the military specification (MIL-STD-1797) given by: $H_m(s) = \frac{0.25}{s^2+0.7s+0.25}$, having state-space representation (A_m, B_m, C_m, D_m)
    - W_e is a low pass filter given by: $W_e(s) = \frac{40(s+10)}{s+0.02}$, having state-space representation $(A_{we}, B_{we}, C_{we}, D_{we})$
  - z_4 represents the scaled output given by $z_4 = y_m T_{rn} W_n$, where:
    - T_{rn} is a matrix with linear independent rows so that one can select the difference $n_{zcp} - n_{zcg}$ from the measured variables vector y_m given by $T_{rn} = [0 \;\; 0 \;\; -1 \;\; 1]$
    - W_n is a low pass filter given by $W_n(s) = \frac{1.34e{-}5(s+100)}{s+6.67}$, having state-space representation $(A_{wn}, B_{wn}, C_{wn}, D_{wn})$
- The measured variables are: θ_{com}, y_m given by the vector $y_m = \left[q, \theta, n_{zcg}, n_{zcp}\right]^T$
    - The loop-shaping transfer function $W(s) = I_2$, given the resulting system $G_s(s) = GW$, having state-space representation (A_s, B_s, C_s, D_s)

The resulting generalized system with respect to NLCF is given by

$$T(s) \coloneqq \begin{bmatrix} A_T & \vdots & B_1 & B_2 \\ \cdots & \cdots & \cdots & \cdots \\ C_1 & \vdots & D_{11} & D_{12} \\ C_2 & \vdots & D_{21} & D_{22} \end{bmatrix} = \left[\begin{array}{cccc:c:cc:c} A_s & 0_{10x2} & 0_{10x1} & 0_{10x1} & \vdots & 0_{10x1} & -H & \vdots & B_s \\ 0_{2x10} & A_m & 0_{2x1} & 0_{2x1} & \vdots & B_m & 0_{2x4} & \vdots & 0_{2x2} \\ B_w T_r C_s & -B_w C_m & A_w & 0_{1x1} & \vdots & 0_{1x1} & B_w T_r & \vdots & B_w T_r D_s \\ B_{wn} T_{rn} C_s & 0_{1x2} & 0_{1x1} & A_{wn} & \vdots & 0_{1x1} & B_{wn} T_{rn} & \vdots & B_{wn} T_{rn} D_s \\ \cdots & \cdots & \cdots & \cdots & \cdots & \cdots & \cdots & \cdots & \cdots \\ & C_s & 0_{4x4} & & \vdots & 0_{4x1} & I_4 & \vdots & D_s \\ & 0_{2x14} & & & \vdots & 0_{2x1} & 0_{2x4} & \vdots & W_z \\ D_w T_r C_s & -D_w C_m & C_w & 0_{1x1} & \vdots & 0_{1x1} & D_w T_r & \vdots & D_w T_r D_s \\ D_{wn} T_{rn} C_s & 0_{1x2} & 0_{1x1} & C_{wn} & \vdots & 0_{1x1} & D_{wn} T_{rn} & \vdots & D_{wn} T_{rn} D_s \\ \cdots & \cdots & \cdots & \cdots & \cdots & \cdots & \cdots & \cdots & \cdots \\ & 0_{1x14} & & & \vdots & & I_1 \quad 0_{1x4} & \vdots & 0_{1x2} \\ & C_s & 0_{4x4} & & \vdots & & 0_{4x1} \quad I_4 & \vdots & D_s \end{array}\right], \quad (8)$$

where

$$H \coloneqq -(ZC_s^T + B_s D_s^T)(I_4 + D_s D_s^T)^{-1}, \quad (9)$$

$Z > 0$ denoting the stabilizing solution of the filtering algebraic Riccati equation:

$$(A_s - B_s(I_4 + D_s D_s^T)^{-1} D_s^T C_s)Z + Z(A_s - B_s(I_4 + D_s D_s^T)^{-1} D_s^T C_s)^T - ZC_s^T(I_4 + D_s D_s^T)^{-1} C_s Z + B_s(I_4 + D_s D_s^T)^{-1} B_s^T = 0. \quad (10)$$

One can check that the solvability conditions of the H_∞ control problem are accomplished. Indeed, the pairs (A_T, B_2) and (C_2, A_T) are stabilizable and detectable, respectively, and the systems (A_T, B_2, C_1, D_{12}) and (A_T, B_1, C_2, D_{21}) have no transmission zeros on the imaginary axis. Moreover, the obtained H_∞ control problem is nonsingular since $D_{12}^T D_{12}$ and $D_{21} D_{21}^T$ are invertible.

Thus, using "*hinfsyn*" procedure in MATLAB, resulting in the control system K_{inf} of order 14, which is determined such that it stabilizes the configuration and minimizes the H_∞ norm of the mapping, $\begin{bmatrix} \theta_{com} \\ w_1 \\ w_2 \end{bmatrix} \rightarrow \begin{bmatrix} z_1 \\ z_2 \\ z_3 \\ z_4 \end{bmatrix}$.

4. Linear simulation analysis

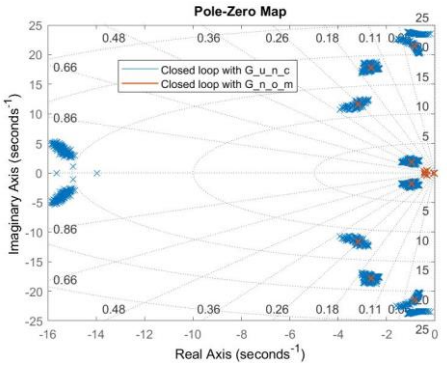

(a) Pole-Zero Map of the closed loop system

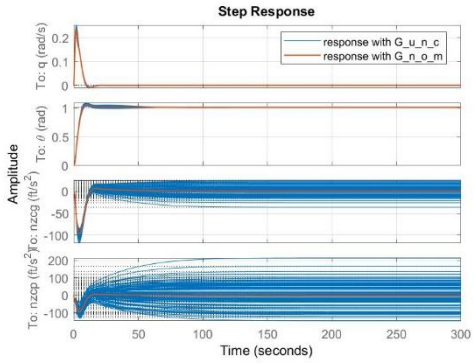

(b) $y_m(t)$ response from θ_{com} step command

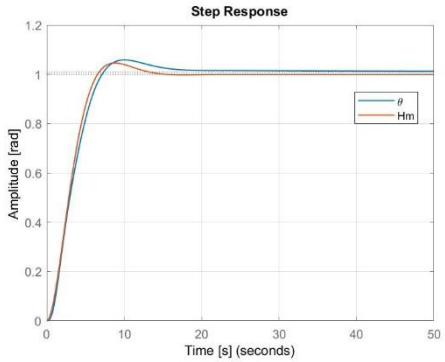

(c) θ tracking of H_m for $\theta_{com} = 1\ [rad]$ using plant $G_{nom}(s)$

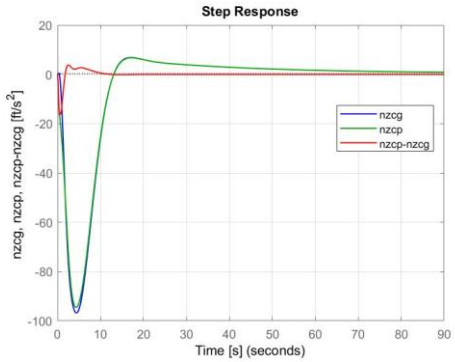

(d) n_{zcg}, n_{zcp} and $n_{zcp} - n_{zcg}$ for $\theta_{com} = 1\ [rad]$ using plant $G_{nom}(s)$

Fig. 7 Results for the closed loop system

As one can see in Fig. 7(a) the resulting closed loop system using the linear nominal plant $G(s)$ maintains stability and so does the closed loop when the linear plant affected by $\pm 10\%$ uncertainties $G_{unc}(s)$ is used (here one can see results for 100 sample systems inside the considered interval). The results in Fig. 7(b) are purely theoretical because the given step command for θ_{com} is in radians and this command is not feasible at the considered flight conditions where the linearization was made. Thus, $n_{zcp}[ft/s^2]\ and\ n_{zcg}[ft/s^2]$ will not reach those values in reality. Their behavior closest to reality can be seen in the next chapter here the nonlinear model was used. Both Fig. 7(b) and 7(c) show that $\theta(t)$ maintains stability and achieves tracking error minimization for all uncertain systems considered in the chosen uncertainty domain. One can notice from Fig. 7(d) that difference $n_{zcp}(t) - n_{zcg}(t)$ reaches near zero values very fast (approx. 15 *sec*) only for the nominal case, but in the uncertainties case the results are not that great when it comes to keeping this difference to a minimum. Nevertheless, stability is maintained for all uncertain systems considered and one can see that now no more ripples can be sensed in the cockpit location in the first 10 *sec* and the transition is much smoother.

In the following the stability robustness proprieties of the proposed controller is addressed. The transfer function used here refers to the θ channel ($\theta_{com} \to \theta$) in open loop. When using the nominal plant in the open loop the resulting robustness is given by: $GM_{nom} = 20.94\ [dB]; PM_{nom} = 46.118\ [deg]; DM_{nom} = \frac{PM_{nom}}{Wcp_{nom}} \frac{pi}{180} = 2.0158\ [sec]$.

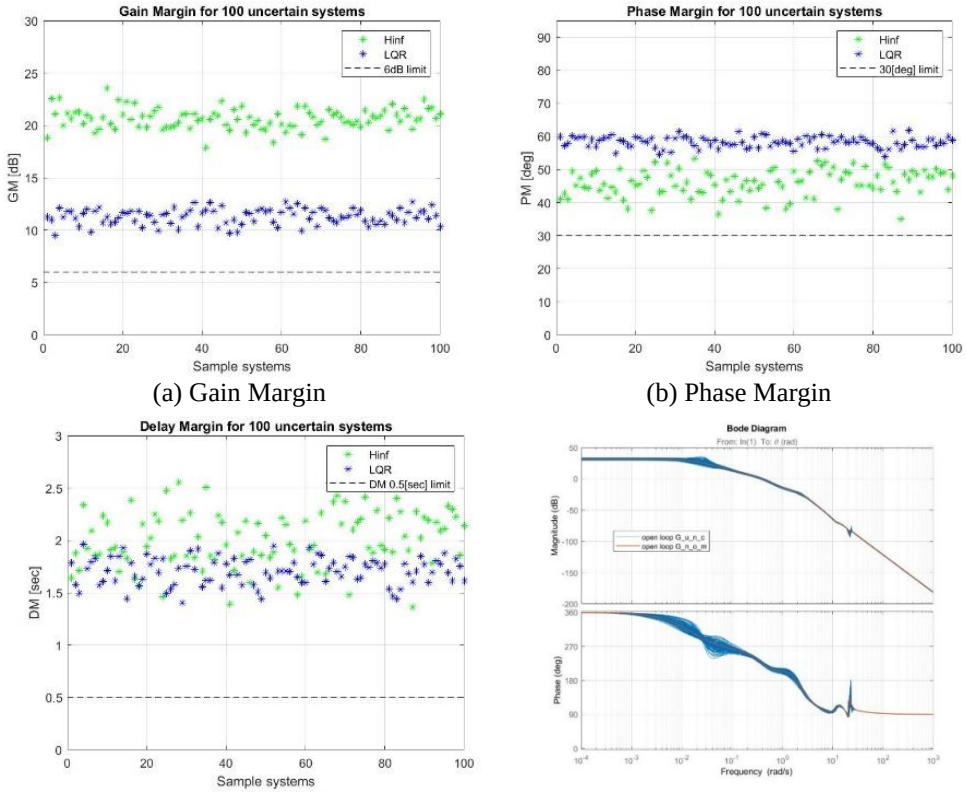

(a) Gain Margin (b) Phase Margin

(c) Delay Margin (d) Bode diagram

Fig. 8 Robustness analysis for 100 open loop sample systems

From Fig. 8 one can see that the gain margin is well above the critical limit of $6\,[dB]$, while the phase margin is maintained above the limit of $30\,[deg]$ resulting in the delay margin being above the limit of $0.5\,[sec]$ for all 100 uncertain plants considered.

5. Nonlinear simulations

The resulting controller computed for the linear system and tested with uncertainties will be tested on the full nonlinear elastic dynamics of the Rockwell B-1 aircraft. The SIMULINK aircraft model corresponds to the description given in [1]. For comparison purpose a simple LQR controller was designed (under the assumption that all states are available, which can be achieved by additionally designing a Kalman filter to estimate the states) in order to keep the pitch angle using the control input δ_{Hc} while the control input δ_{cvsym} was used to filter the difference $n_{zcp} - n_{zcg}$ with the same filter used in [1].

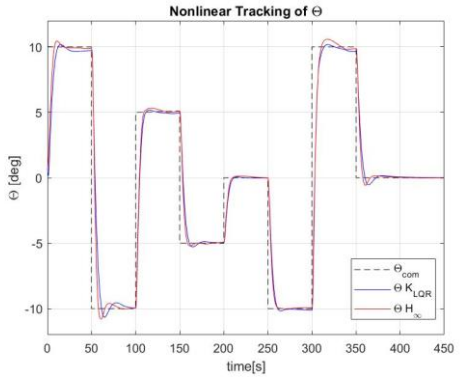

(a) Controlled pitch attitude

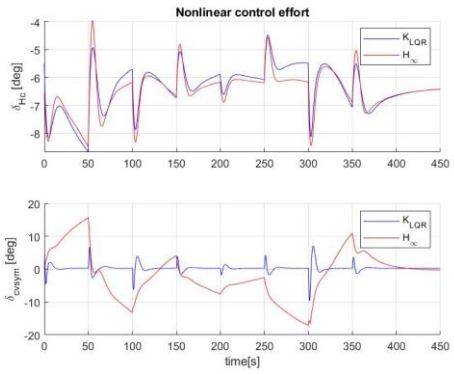

(b) Control effort

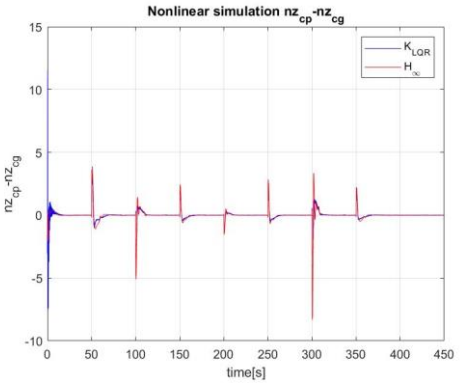

(c) Effect of the flexible modes

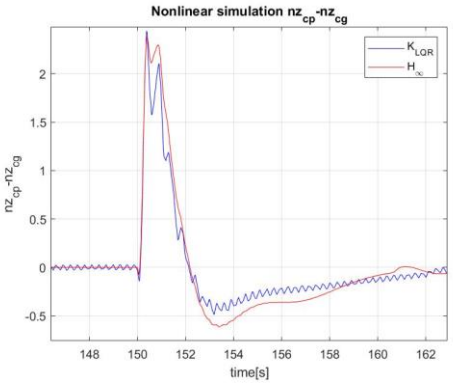

(d) Effect of the flexible modes for ~10 *sec*

Fig. 9 Nonlinear simulation for the nominal case of all proposed controllers

The difficulty when working with nonlinear model is that things might not work properly for long simulation running times because coupling between longitudinal and lateral channels can interfere resulting in instability. Thus, in order to avoid instability, a simple lateral-directional gain schedule controller was developed so that the lateral dynamics are kept to their trim state for the duration of the simulation. Also, the flexible modes for the lateral channel were turned off.

The nonlinear simulation took place for 450 *sec* while the desired pitch attitude was given by several doublet commands. One can notice in Fig. 9(a) that the commanded pitch is chosen between $\pm 10\ deg$ and steady state was reached for both controllers with approximately the same transient time and overshot. The time response of the control effort represented in Fig. 9(b) is relatively similar in all cases for δ_{Hc}, but for δ_{cvsym} differs for each controller. The difference $n_{zcp}(t) - n_{zcg}(t)$ has some ripples in the LQR+filter case as one can see in Fig. 9(d), but in the H_∞ case there are almost no ripples present. This difference was maintained to a low level during the proposed simulation inside the interval $(-8ft/s^2, 4ft/s^2)$ as can be noticed in Fig 9(c). Although not individually represented here the normal accelerations sensed in the cockpit n_{zcp} and in the center of gravity n_{zcg} both tend to $0ft/s^2$ when steady state is reached.

6. Conclusions and future work

Combining the two control surfaces in order to achieve both control objectives simultaneously, as the H_∞ design does, was proven to give more satisfactory results when working with flexible modes, as compared to acting on separate control channels (the first to achieve attitude tracking and the second to compensate for the flexible modes effects).

The main difficulty of this approach is trying to attenuate the effects of the high frequency elastic modes while achieving low frequency control objectives. Thus, the design main focus was achieving the low frequency control objectives, but adjustments were made in order to reduce elasticity effect as much as possible.

Future work involves a new control design for the lateral-directional dynamics of the Rockwell B-1 nonlinear model.

Acknowledgement

This work has been funded by the European Social Fund from the Sectoral Operational Programme Human Capital 2014-2020, through the Financial Agreement with the title *"Scholarships for entrepreneurial education among doctoral students and postdoctoral researchers (Be Antreprenor!)"*, Contract no. 51680/09.07.2019 - SMIS code: 124539.

R E F E R E N C E S

[1] *Dr. David K. Schmidt*, "A Non-Linear Simulink Simulation Of a Large, Flexible Aircraft - FLEXSIM," March 17, 2013.

[2] J. *H. Wykes, A. S. Mori and C. J. Borland*, "B-1 Structural Mode Control System", 4th Aircraft Design, Flight Test, and Operations Meeting, Aircraft Design and Operations Meetings, Los Angeles,U.S.A, 1972.

[3] *J. Wykes, C. J. Borland, M. Klepl, and C. MacMiller*, "Design and development of a structural mode control system", NASA/CR, 143846, 1977.

[4] *Doyle, John C. and Glover, Keith and Khargonekar, Pramod P. and Francis, Bruce A*, "State-space solutions to standard H_2 and H_∞ control problems". IEEE Transactions on Automatic Control, 34 (8). pp. 831-847. ISSN 0018-9286, 1989.

[5] *Adrian-Mihail STOICA*, "Disturbance attenuation and its applications", ISBN 973-27-1057-8, Editura Academiei Romane 2004.

[6] *T. Iwasaki and R. E. Skelton*, "All Controllers for the General H_∞ Control Problem: LMI Existence Conditions and State Space Formulas". Automatica, Vol. 30, No. 8, pp. 1307-1317, 1994.

[7] *Duncan C. McFarlane and Keith Glover*, "Robust controller design using normalized coprime factor plant descriptions". ISBN 3-540-51851-7, Springer-Verlag Berlin Heidelberg, NewYork, 1990.

[8] *Zhou, K., and J.C. Doyle*, "Essentials of Robust Control". NY: Prentice-Hall, 1998.

[9] F. *L. Lewis and V. L. Syrmos*, "Optimal Control", Wiley, second edition, 1995.

[10] *Boyd, S., Ghaoui, L.E., Feron, E. and Balakrishnan, V*, "Linear Matrix Inequalities in System and Control Theory". SIAM Studies in Applied Mathematics, Philadelphia, USA. 1994.

[11] *Martin R. Waszak, John B. Davidson and David K. Schmidt*, "A Simulation Study of the Flight Dynamics of Elastic Aircraft.", Volume Two-Data, NASA CR-4102, december, 1987.